Accepted Manuscript

Effects of passive hydrodynamics force on harmonic and chaotic oscillations in nonlinear chemical dynamics

D.L. Olabodé, C.H. Miwadinou, V.A. Monwanou, J.B. Chabi Orou

PII: S0167-2789(18)30073-3
DOI: https://doi.org/10.1016/j.physd.2018.09.001
Reference: PHYSD 32046

To appear in: *Physica D*

Received date : 11 February 2018
Revised date : 2 August 2018
Accepted date : 4 September 2018

Please cite this article as: D.L. Olabodé, et al., Effects of passive hydrodynamics force on harmonic and chaotic oscillations in nonlinear chemical dynamics, *Physica D* (2018), https://doi.org/10.1016/j.physd.2018.09.001

Effects of Passive Hydrodynamics Force on Harmonic and Chaotic Oscillations in Nonlinear Chemical Dynamics

D. L. Olabodé[a], C. H. Miwadinou[a,b,*], V.A. Monwanou[a], J.B. Chabi Orou[a]

[a]*Laboratoire de Mécanique des Fluides, de la Dynamique Nonlinéaire et de la Modélisation des Systèmes Biologiques* **(LMFDNMSB)***; Institut de Mathématiques et de Sciences Physiques, Porto-Novo, Bénin*

[b]*Département de Physiques, Ecole Normale Supérieure (ENS) Natitingou, Université Nationale des Sciences, Technologiques, Ingénierie et Mathématiques (UNSTIM) Abomey, Bénin*

Abstract

This work studies the nonlinear dynamics and passive control of chemical oscillations governed by a forced modified Van der Pol-Duffing oscillator. We considered the dynamics of nonlinear chemical systems subjected to fluctuating hydrodynamic drag forces. The computation of fixed points of the nonlinear chemical system is made in detail by utilizing Cardan's method. The harmonic balance method is used to find the amplitudes of the oscillatory states. The Floquet theory and the Whittaker method are utilized to analyze and analytically determine the stability boundaries of oscillations. The influences of system parameters in general and in particular the effect of the parameter K and the constraint parameter β which shows the difference between a nonlinear chemical dynamics order two differential equation and ordinary Van der Pol-Duffing equation are observed on the state of the second stability criterion. The effects of the control process on chaotic dynamics states are investigated through bifurcations structures, Lyapunov exponent, phase portraits and Poincaré section. The results obtained by the analytical methods are validated and complemented by the results of numerical simulations.

*Corresponding author

Email address: `hodevewan@yahoo.fr, clement.miwadinou@imsp-uac.org, BP:763 Porto-Novo/Bénin` (C. H. Miwadinou)

Keywords: Passive control, Nonlinear dissipative chemical dynamics, Forced modified Van der Pol-Duffing oscillator, Bifurcation, Chaos.

1. Introduction

In several scientific domains ranging from physics, engineering, chemistry, biochemistry to biology, the study of nonlinear oscillators is of increasing interest in recent years. The chemical oscillating reactions in a continuously stirred tank reactor (CSTR) is one of the first biochemical oscillations discovered. Considerable theoretical progress on the nature of chemical oscillation, the only known chemical oscillators were either biological in origin, like the glycolytic and oxidase-peroxidase systems; discovered accidentally, like the Bray and BZ reactions; or variants of those reactions [1, 2, 3, 4, 5, 6, 7, 8]. In these chemical oscillations various dynamics behaviors are studied by many researchers. For instance, nonequilibrium phenomena such as oscillations, bistability, complex oscillations, and quasi-chaotic behavior of the reaction are revealed by these studies. One of the main challenges has been to predict and to control these phenomena in nonlinear chemical oscillations for potential applications (see [1, 2, 3, 4, 5, 6, 7, 8]). In order to understand the biochemistry complex dynamics, Duffing-Van der Pol-Rayleigh oscillators have been used and studied by many researchers [9, 10, 11, 12]. The most interesting nonlinear oscillators are self-excited, and the study of their dynamics is often difficult. Nowadays, these oscillators are combined in the modeling of complex systems to better understand the dynamics of these systems [13, 14]. For the control process, passive, active, semi-active controls are often used depending to the nature of the problem and system under consideration. An exhaustive review of the description and most important results of active control are given in Ref. [15, 16, 17, 18, 19]. When it comes to biochemical oscillations such as the case of glycolytic oscillations in yeast, control of oscillations has been achieved through the substrate injection rate [20, 21]. For instance, the reduction of the injection rate causes a lengthening of the oscillations period while a decreasing of the injection rate be-low a given threshold causes the reversible suppression of oscillations. Here, we utilize a new approach via passive control [22] which unlike the active control scheme, do not require the use of, actuators, sensors, computation of control laws and external power supplies and therefore is cost efficient in the energy view point. We will also determine the range of control parameters which leads to a good control.

The organization of this paper is as follows. In Section 2, we give the mathematical modeling of nonlinear chemical oscillations and we formulate the passive control process. In Section 3, we check the equilibrium points of the autonomous system and the amplitude of forced oscillatory states. The stability boundaries is analyzed and the effect of the different parameters of the model under consideration on the amplitude of harmonic resonance are investigated. Section 4 deals with routes to chaotic behavior and effect of the control process on chaotic dynamics states. The conclusion is presented in the last section.

2. Model and equation of oscillations

In this work, we consider all nonlinear chemical systems as a kinetic example which can be described by the following equations [1, 3, 8]

$$A \xrightarrow{k_1} X, \tag{1}$$

$$B + X \xrightarrow{k_2} 2X, \tag{2}$$

$$D + X \xrightarrow{k_3} products, \tag{3}$$

$$X \xrightarrow{k_4} X', \tag{4}$$

$$B + X' \xrightarrow{k_5} Y, \tag{5}$$

$$Y \xrightarrow{k_6} X' + products. \tag{6}$$

Based upon the laws of mass action and conservation and assuming that the sink of the product is a first order reaction, the self-oscillations in somes nonlinear chemical systems can be described by the mathematical model defined as follows:

$$\frac{dx}{dt} = -(x^3 - \mu_0 x + \lambda) - ky. \tag{7}$$

$$\frac{dy}{dt} = \frac{x-y}{\kappa} \tag{8}$$

where $\mu_0 > 0$, λ is the constraint parameter, k a second constraint parameter on which feedback values depend, and κ the characteristic evolution time of the feedback. x and y designate the concentrations of X and Y respectively. Several researchers have already studied the nonlinear chemical systems modeled by Eq.(8). A variety of nonlinear phenomena such as multistability, bifurcations and chaotic behavior is observed when the reactive species come into contact with the catalytic surface. Many researches have proved that these complex phenomena can be analyzed from the modeling of nonlinear chemical systems by nonlinear oscillators equations [9, 10, 11, 12]. For example, Van der Pol oscillator can be used to model a self-excited biological system based on enzymes-substrates reactions [10]. In the same vein, we seek to reduce the number of species needed to control the dynamics of chemical reactions governed by Eq. (8). Thus, differentiating this equation and eliminating y, the system equation can be transformed after some algebraic manipulations in the following single second order differential equation [23]:

$$\ddot{\zeta} + \mu(1-\zeta^2)\dot{\zeta} + \alpha\zeta + \gamma\zeta^3 + \beta = 0, \tag{9}$$

where

$$\zeta = ax, \qquad a = \sqrt{\tfrac{3\kappa}{1+\mu_0\kappa}}, \qquad \mu = \tfrac{\mu_0\kappa+1}{\kappa},$$
$$\alpha = \tfrac{k-\mu_0}{k}, \qquad \beta = \tfrac{\lambda a}{\kappa}, \qquad \gamma = \tfrac{\mu_0\kappa+1}{3\kappa^2}.$$

The literature provied that a richness of complex dynamics behaviors can be obtained when dissipative self-oscillators are submitted to external forcing. Often, the external force field is used in the simplest periodic forcing form. this external force field can be seen as exposure of the system to a source of periodic radiation, which affects the production of one of the two species or excites its reactivity. In this work, the main investigation concerns how this periodic perturbation can modify the dynamics of the chemical systems. The output of the reactive system is modified only by applying a simple periodic external force. This is technologically important because we don't need to fabricate sophisticated catalytic materials or to apply specific experimental conditions [24]. By assuming that the model is subjected to an external sinusoidal excitation $F\cos\Omega t$, Eq. (9) becomes a nonlinear single second order differential equation on the form

$$\ddot{\zeta} + \mu\left(1-\zeta^2\right)\dot{\zeta} + \alpha\zeta + \gamma\zeta^3 + \beta = F\cos\Omega t. \tag{10}$$

When the model is also influenced by fluctuating hydrodynamic drag forces [22], the equation of the system under such a control scheme becomes

$$\ddot{\zeta} + \mu(1-\zeta^2)\dot{\zeta} + \alpha\zeta + \gamma\zeta^3 + \beta = F\cos\Omega t - \epsilon K(U-\dot{\zeta})\left|U-\dot{\zeta}\right| \tag{11}$$

where ζ, $\dot{\zeta}$ and $\ddot{\zeta}$ are the displacement, velocity and acceleration respectively. μ, α and γ respectively denote the damping coefficient, linear and cubic nonlinear restoring parameters. F and Ω are respectively the amplitude and the frequence of the excitation. U is the fluid speed, K and $(U-\dot{\zeta})^2$ stand for the control gain coefficient and the fluid speed relative to the velocity respectively. The control system can then be written as follows:

$$\ddot{\zeta} + \mu(1-\zeta^2)\dot{\zeta} + \alpha\zeta + \gamma\zeta^3 + \beta = F\cos\Omega t - \epsilon K(U-\dot{\zeta})^2, \epsilon = \pm 1 \tag{12}$$

For the particular case where the constraint parameter $\lambda = 0$, the constant therm $\beta = 0$ and if $\epsilon = 0$, Eq.(12) is reduced to the equation of classical Van der Pol-Duffing oscillator. The passive hydrodynamics drag forces follow the positive direction of flow velocity in the case where $\epsilon = +1$ and are opposite of flow velocity when $\epsilon = -1$.

3. Harmonic oscillations states

3.1. Equilibrium points of autonomous system

In this part, we determine the equilibrium points of the autonomous nonlinear chemical system under passive control and we analyze their stability. In this order, we write the equation of autonomous system as follow

$$\dot{\zeta} = u \tag{13}$$

$$\dot{u} = -\mu(1-\zeta^2)u - \alpha\zeta - \gamma\zeta^3 - \beta - \epsilon K(U-u)^2. \tag{14}$$

All equilibrium points of the autonomous system verify:

$$u = 0, \qquad \gamma\zeta^3 + \alpha\zeta + \beta + \epsilon K U^2 = 0. \tag{15}$$

Using the Cardan method [25] to solve Eq.(15), we rewrite this equation in the form:

$$\zeta^3 + p\zeta + q = 0, \tag{16}$$

where $p = \frac{\alpha}{\gamma}$ and $q = \frac{\beta+\epsilon K U^2}{\gamma}$. The associate characteristic equation is

$$T^2 + qT - \frac{p^3}{27} = 0 \tag{17}$$

The equilibrium points of system depend on the parameters of the system and therefore the sign of D with

$$D = 27\Delta' = 4p^3 + 27q^2, \tag{18}$$

where Δ' represents the determinant of Eq. (17). The value of α seriously influences the sign of D because the parameter $\gamma > 0$ for the chemical system modeled by Eq. (12).

Thus, if $\alpha > 0$ the parameter $D > 0$ and the system has one fixed point that is an unstable focus regardless of the values of the other parameters. For example, when $\alpha = 0.5$; $\gamma = 0.05$; $\mu = 0.04$; $\beta = 0.05$; $\epsilon = 1$; $K = 0.1$; $U = 0.3$, $D = 4037,5948 > 0$ and the equilibrium point is $P_0^+(\zeta_0 = -0.1178363795, 0)$. The Eigenvalues of Jacobian matrix of the system at P_0^+ are $\lambda_1 = 0.01027770825 - 0.7085034796i$; $\lambda_2 = 0.01027770825 + 0.7085034796i$. We note that the real part of these complex conjugates eigen values is positive and the equilibrium point P_0 is unstable focus. Fig.(1) shows the phase space and the times histories of the autonomous system and we note that the amplitude of chemical oscillations increases with the time and confirm that the only equilibrium point is unstable focus. For the same values of the parameters of the system, and $\epsilon = -1$, $D = 4018, 1548 > 0$ and the fixed point is $P_0^-(\zeta_0 = -0.08194497441, 0)$. The two eigenvalues of Jacobian matrix of the system at P_0^- are $\lambda_1 = -0.04986570043 - 0.7060599541i$; $\lambda_2 = -0.04986570043 + 0.7060599541i$. We conclude that the fixed point is stable focus. We plot in Fig.(2) the phase space and its corresponding times histories. Through these figures, it is noted that the amplitude of chemical oscillations decreases in time and confirms that the equilibrium point is a stable focus.

Now, we consider $\alpha < 0$ and we analyze the all sign of D. The autonomous system can present one, two or three equilibrium points (ζ_n, u_n). The eigenvalues of the corresponding Jacobian matrix at each of the equilibrium points are determined by solving

$$\lambda^2 + \lambda a_1 + a_2 = 0, \tag{19}$$

with

$$a_1 = \mu - \mu\zeta_n^2 - 2\epsilon KU; \quad a_2 = \alpha + 3\gamma\zeta_n^2$$

- If $D > 0$, the autonomous system has one equilibrium point $P(\zeta_0, 0)$ with

$$\zeta_0 = (-\frac{q}{2} - (\frac{q^2}{4} + \frac{p^3}{27})^{\frac{1}{2}})^{1/3} + (-\frac{q}{2} + (\frac{q^2}{4} + \frac{p^3}{27})^{\frac{1}{2}})^{1/3}.$$

For example when $\alpha = -0.3$; $\gamma = 0.05$; $\mu = 0.07$; $\beta = 0.0647$; $\epsilon = -1$; $K = 0.3$ and $U = 1.75$, $D = 7013.535147 > 0$ and the fixed point is $(\zeta_0 = 3.334940789, u_0 = 0)$. The eigenvalues at this equilibrium point are $\lambda_1 = -0.1707359477 - 1.157205144i$; $\lambda_2 = -0.1707359477 + 1.157205144i$, and prove that the equilibrium point is the stable focus and confirmed by the phase space and its corresponding times histories plotted in Fig.(3).

- If $D < 0$ and $\alpha < 0$, we have three equilibrium points given by

$$\zeta_n = 2\sqrt{-\frac{p}{3}}\cos[\frac{1}{3}\arccos(-\frac{q}{2}\sqrt{-\frac{27}{p^3}}) + \frac{2n\pi}{3}], \tag{20}$$

$$\dot{\zeta}_n = 0, n = 1, 2, 3, \tag{21}$$

1. When $a_1^2 - 4a_2 > 0$, we have two real values

$$\lambda_1 = -\frac{a_1}{2} - \frac{1}{2}\sqrt{a_1^2 - 4a_2}, \qquad \lambda_2 = -\frac{a_1}{2} + \frac{1}{2}\sqrt{a_1^2 - 4a_2}$$

   (a) If $a_1 > 0, a_1 > \sqrt{a_1^2 - 4a_2}$, the each eigenvalue is negative and the fixed point is stable node.

   (b) If $a_1 < 0, a_1 < -\sqrt{a_1^2 - 4a_2}$, the eigenvalues are positives and the fixed point is unstable node

   (c) When $a_1 > 0, a_1 < \sqrt{a_1^2 - 4a_2}$, the two eigenvalues have opposite signs and the equilibrium point is saddle node.

2. If $a_1^2 - 4a_2 < 0$, the two eigenvalues are complex conjugates and given by:

$$\lambda_1 = -\frac{a_1}{2} - i\frac{1}{2}\sqrt{-a_1^2 + 4a_2}, \qquad \lambda_2 = -\frac{a_1}{2} + i\frac{1}{2}\sqrt{-a_1^2 + 4a_2}.$$

   Thus, the equilibrium point is a stable focus if $a_1 > 0$, unstable focus if $a_1 < 0$ and a center when $a_1 = 0$.

3. If $a_1^2 = 4a_2$ we have $\lambda_1 = \lambda_2 = -\frac{a_1}{2}$. The equilibrium point is stable when $a_1 > 0$ and unstable when $a_1 < 0$.

In order to verify our analytical predictions, we consider for example $\alpha = -0.3$; $\gamma = 0.05$; $\mu = 0.07$; $\beta = 0.0647$; $\epsilon = -1$; $K = 0.3$; $U = 0.50$. For these parameters, $D = -862.854228 < 0$ and the three equilibrium points are $P_1(\zeta_1 = -2.432139161, \dot{\zeta}_1 = 0)$, $P_2(\zeta_2 = -0.03434008254, \dot{\zeta}_2 = 0)$ and $P_3(\zeta_3 = 2.466479244, \dot{\zeta}_3 = 0)$. For the fixed point P_1, $a_1 = -0.04407106289$ and $a_2 = 0.5872951348$, the eigenvalues are $\lambda_1 = 0.022035533145 - 0.7660349667i$; $\lambda_2 = 0.022035533145 + 0.7660349667i$ and P_1 is unstable focus. For P_2, $a_1 = 0.3699174531$ and $a_2 = -0.2998231138$, the two eigenvalues are $\lambda_1 = -0.7629144725$; $\lambda_2 = 0.3929970194$ and P_2 is the saddle node. For P_3, $a_1 = -0.05584639028$

and $a_2 = 0.6125279792$, $\lambda_1 = 0.02792319514 - 0.7821433847i$; $\lambda_1 = 0.02792319514 + 0.7821433847i$ and the equilibrium point is unstable focus (Fig.(4)).

• If $D = 0$, our autonomous system has two equilibrium points; one is simple and other is degenerate. The simple equilibrium point is ($\zeta_1 = \frac{3q}{p}, u_1 = 0$) and the degenerate equilibrium point is ($\zeta_2 = \zeta_3 = -\frac{3q}{2p}, u_2 = u_3 = 0$). To illustrate this analytical result, we take $\alpha = -0.3$; $\gamma = 0.05$; $\mu = 0.07$; $\beta = 0.0647$; $\epsilon = -1$; $K = 0.3475427125$; $U = 1$ and we have $D = 0$; the simple fixed point is ($\zeta_1 = 2.828427125, u_1 = 0$) and the degenerate fixed point is ($\zeta_2 = -1.414213563, u_2 = 0$). For the simple equilibrium point, $a_1 = 0.2050854249$ and $a_2 = 0.9000000002$, the eigenvalues are $\lambda_1 = -0.1025427125 - 0.9431251201i$; $\lambda_2 = -0.1025427125 + 0.9431251201i$, and this equilibrium point is stable. For the degenerate point, $a_1 = 0.6250854249$ and $a_2 = 2.6595 * 10^{-10}$, the two eigenvalues are $\lambda_1 = -0.6250854245$; $\lambda_2 = -4.089096 * 10^{-10}$, thus this equilibrium point is a stable node.

3.2. Amplitude of forced oscillatory states

When the fundamental component of the solution and the external excitation have the same period, the amplitude of harmonic oscillations can be determined using the harmonic balance method [26, 27]. For this purpose, we express its solutions in the following form

$$\zeta = A\cos(\Omega t + \phi) + A_0 \tag{22}$$

where A and A_0 are the amplitudes of oscillations. We introduce the solution Eq.(22) in Eq.(12) and equate the constants and the coefficients of $\sin\Omega t$ and $\cos\Omega t$. By hypothesizing that $|A_0| \ll |A|$, i.e that shift in $\zeta = 0$ is small compared to the amplitude, then A_0^2 and A_0^3 terms can be neglected, we determine that the amplitude of harmonic oscillatory states under the control process satisfies the following set of algebraic equations:

$$A_0 = -\frac{2\beta + 2\epsilon K U^2 + \epsilon K A^2 \Omega^2}{2\alpha + 3\gamma A^2}, \tag{23}$$

$$[(\alpha - \Omega^2)A + \frac{3}{4}\gamma A^3]^2 + [(2\epsilon K U\Omega - \mu\Omega)A + \frac{1}{4}\mu A^3 \Omega]^2 - F^2 = 0. \tag{24}$$

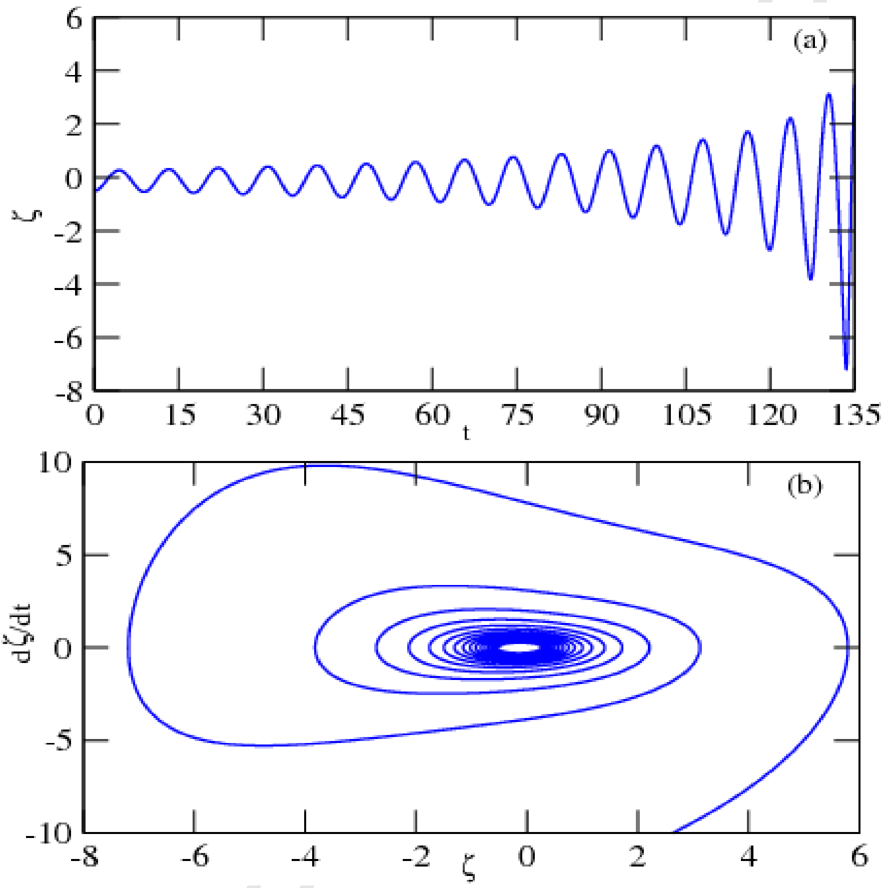

Figure 1: Time histories (a) and phase portrait (b) of instable autonomous oscillations for $\alpha = 0.5$; $\gamma = 0.05$; $K = 0.1$; $U = 0.3$; $\mu = 0.04$; $\beta = 0.05$ and $\epsilon = 1$.

We solved Eq. (24) using the Newton-Raphson algorithm. A good agreement is obtained for comparison between the analytical frequency response curve obtained via Eq. (24) and the one provided by numerical computation of Eq. (12) (see Fig. 5). We investigated the effects of the passive control on the resonance state, process of hysteresis and amplitude jump, the cancellation of these phenomena has been successfully achieved. Fig. 6 illustrate the effect of the parameter ϵ on the amplitude of harmonic oscillation. Through this figure, it is noted that the amplitude of harmonic resonance is reduced for

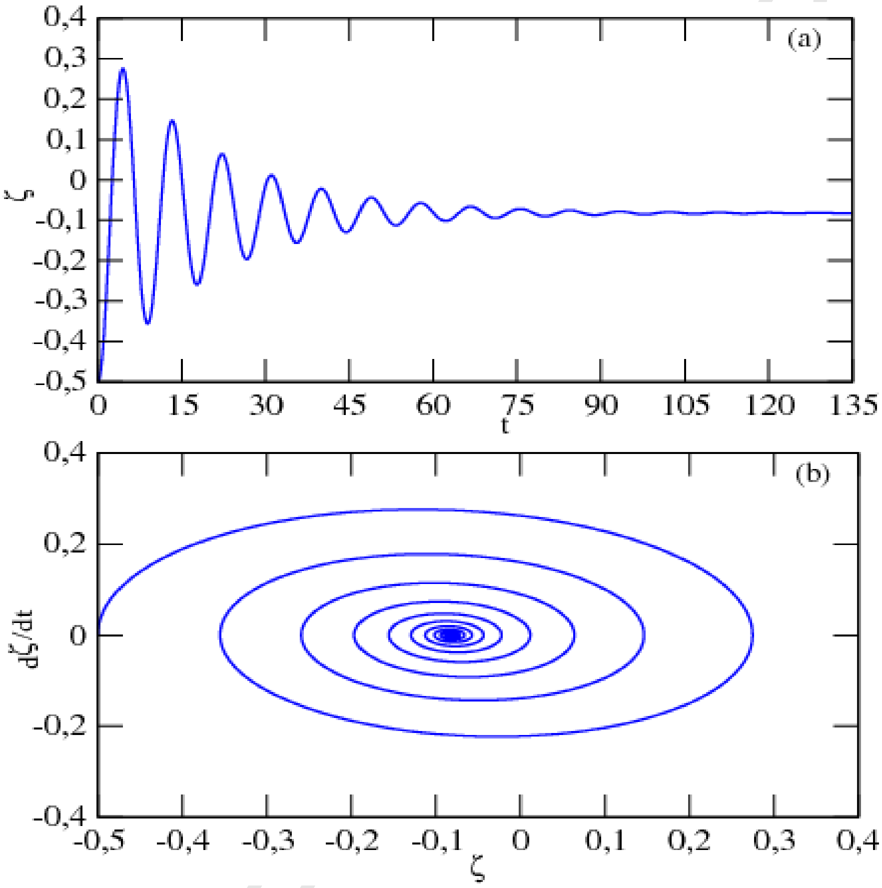

Figure 2: Time histories (a) and phase portrait (b) of stable autonomous oscillations for $\alpha = 0.5$; $\gamma = 0.05$; $K = 0.1$; $U = 0.3$; $\mu = 0.04$; $\beta = 0.05$ and $\epsilon = -1$.

the two hydrodynamic force directions when the external excitation $F \leq 0.2$ (see Fig. 6 (a)) but it is the largest for $\epsilon = -1$ when $F > 0.2$ (see Fig. 6 (b)). It is also noticed that the amplitude of resonance increases with F and the unstable amplitude disappears with it (see Fig. 7). We plot in Fig. 8 the effect of the cubic and restoring force and one can observe that as it increases, the harmonic resonance amplitude decreases and the model goes from resonance to a hysteresis state. The effect of damping parameter μ on harmonic resonant state is presented in Fig. 9. Our investigation shows that the harmonic

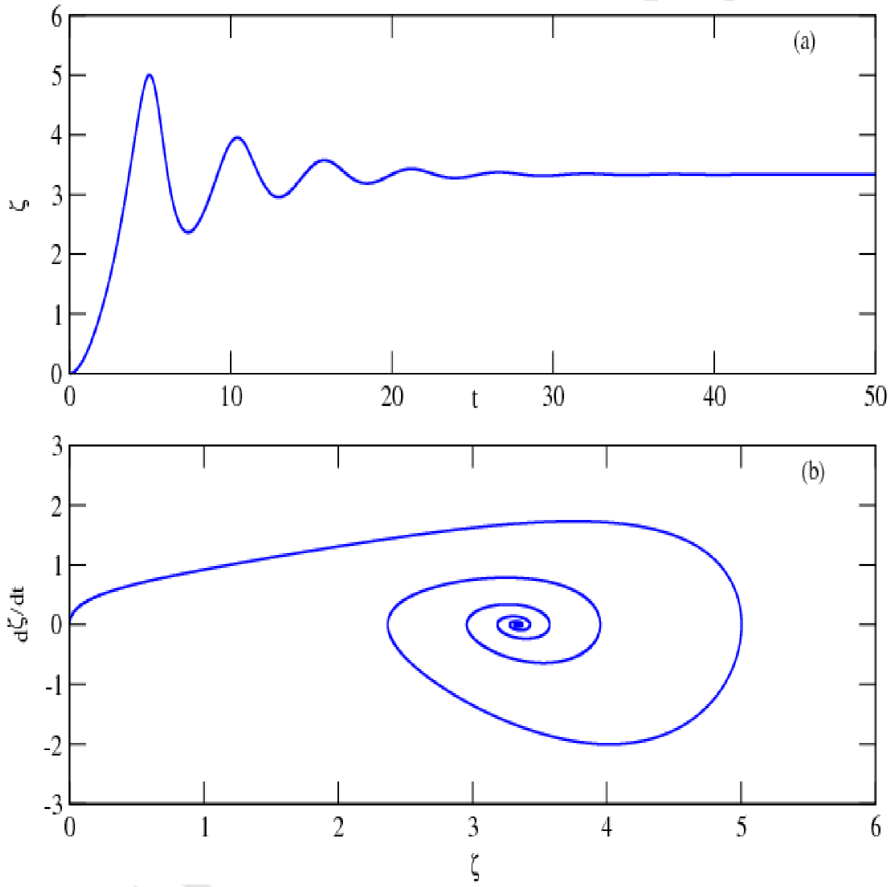

Figure 3: Time histories (a) and phase portrait (b) of the system for $\alpha = -0.3$; $\gamma = 0.05$; $K = 0.3$; $U = 1.75$; $\mu = 0.07$; $\beta = 0.0647$ and $\epsilon = -1$.

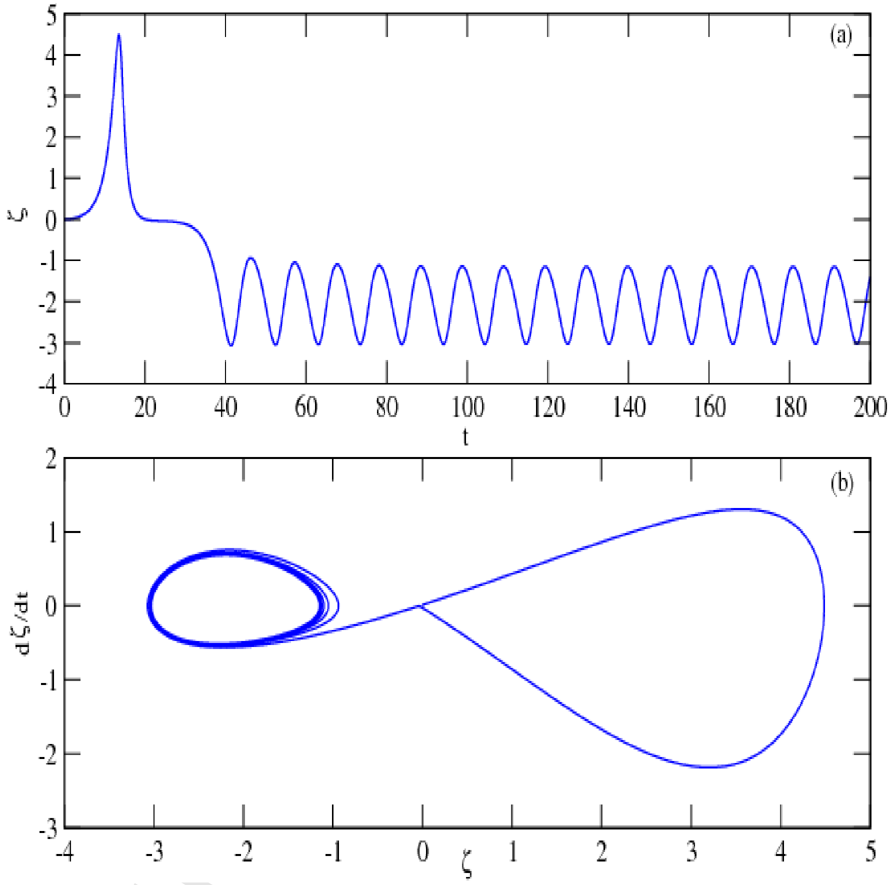

Figure 4: Time histories (a) and phase portrait (b) of the system for $\alpha = -0.3$; $\gamma = 0.05$; $K = 0.3$; $U = 0.5$; $\mu = 0.07$; $\beta = 0.0647$ and $\epsilon = -1$.

resonance amplitude and instability domain increase with μ ranging in $[0, 0.2]$ while the harmonic resonance amplitude decrases and resonance state disappears when the parameter μ decreases remaining greater than 0.2. Fig. 10 shows the effect of control parameter on amplitude-response curves. It is noticed that the hysteresis phenomenon disappears when the passive control force increases. Fig. 10 shows the evolution of the amplitude of harmonic oscillations when the passive control parameters varied. It can be observed that the amplitude of harmonic oscillations decreases when the passive control parameters K and U increase. We can conclude that our passive control is convenient because the amplitude of nonlinear chemical oscillations is considerably reduced when the appropriate control parameters varied.

3.3. Stability boundaries analysis

To analyze the stability of harmonic oscillations in nonlinear chemical dynamics, we used the following linear variational equation derived from Eq.(12):

$$\ddot{\eta} + [\mu(1-\zeta^2) + 2\epsilon K(\dot{\zeta} - U)]\dot{\eta} + (\alpha - 2\mu\zeta\dot{\zeta} + 3\gamma\zeta^2)\eta = 0 \tag{25}$$

where η stands for the perturbation variable. The oscillatory states are stable if η decreases in time. We use the Floquet Theory [26, 27, 22, 14] recognized as a convenient analytical tool to study the stability of oscillations of the system. By setting $\tau = \frac{\Omega t+\phi}{2}$ and using the solution $\zeta(t)$, we rewrite Eq. (25) as follows:

$$\ddot{\eta} + [2L + M(\tau)]\dot{\eta} + N(\tau)\eta = 0, \tag{26}$$

where

$$\begin{aligned}
L &= \frac{1}{\Omega}[\mu(1-\frac{A^2}{2}) - 2\epsilon KU], \qquad (27)\\
M(\tau) &= \Lambda_1 \sin 2\tau + \Lambda_2 \cos 2\tau + \Lambda_3 \cos 4\tau,\\
N(\tau) &= \Gamma_0 + \Gamma_1 \sin 2\tau + \Gamma_2 \cos 2\tau + \Gamma_3 \sin 4\tau + \Gamma_4 \cos 4\tau,
\end{aligned}$$

with

$$\Lambda_1 = -4\epsilon K A, \qquad \Lambda_2 = -\frac{4\mu A A_0}{\Omega}, \qquad \Lambda_3 = -\frac{\mu A^2}{\Omega}$$

$$\Gamma_0 = \tfrac{4}{\Omega^2}[\alpha + \tfrac{3}{2}\gamma A^2], \qquad \Gamma_1 = \tfrac{8\mu A A_0}{\Omega},$$
$$\Gamma_2 = \tfrac{24\gamma A A_0}{\Omega^2}, \qquad \Gamma_3 = \tfrac{4\mu A^2}{\Omega}, \qquad \Gamma_4 = \tfrac{6\gamma A^2}{\Omega^2}.$$

To deepen our discussion of the stability boundaries of the control process, we make use of the following transformation

$$\eta = \upsilon \exp(-L\tau) \exp\{-\frac{1}{2}\int_0^\tau M(\tau')d\tau'\} \tag{28}$$

to bring back Eq.(26) to the following Hill equation [26, 27, 22, 14]

$$\begin{aligned} &\ddot{\upsilon} + [b_0 + 2b_{1s}\sin 2\tau + 2b_{1c}\cos 2\tau + 2b_{2s}\sin 4\tau + \\ &2b_{2c}\cos 4\tau + 2b_{3s}\sin 6\tau + 2b_{3c}\cos 6\tau + 2b_{4c}\cos 8\tau]\upsilon = 0, \end{aligned} \tag{29}$$

where

$$b_0 = \Gamma_0 - L^2 - \tfrac{1}{8}(\Lambda_1^2 + \Lambda_2^2 + \Lambda_3^2),$$
$$b_{1s} = \tfrac{1}{2}[\Gamma_1 + \Lambda_2 - (L - \tfrac{1}{4}\Lambda_3)\Lambda_1],$$
$$b_{1c} = \tfrac{1}{2}[\Gamma_2 - \Lambda_1 - (L + \tfrac{1}{4}\Lambda_3)\Lambda_2],$$

$$b_{2s} = \Lambda_3 - \tfrac{1}{8}\Lambda_1\Lambda_2 + \tfrac{1}{2}\Gamma_3,$$
$$b_{2c} = \tfrac{1}{2}[\Gamma_4 - L\Lambda_3 + \tfrac{1}{8}(\Lambda_1^2 - \Lambda_2^2)],$$
$$b_{3s} = -\tfrac{\Lambda_1\Lambda_3}{8}, \quad b_{3c} = -\tfrac{\Lambda_2\Lambda_3}{8},$$

$$b_{4c} = -\frac{\Lambda_3^2}{16}.$$

The application of the Floquet Theory [26, 27, 22, 14] to Eq.(29) leads to a solution that may be either stable or unstable. We have used the Whittaker method [27] to discuss unstable solutions. Eq. (29) shows that the stability boundaries of the control process are to be investigated around four main parametric resonances defined at $b_0 = n^2$ (with n = 1,2,3,4). So, the solution of Eq.(29) at the nth unstable region may be approximated by the following expression:

$$\eta = exp(\rho\tau)\sin(n\tau - \varphi), \tag{30}$$

where ρ is the characteristic exponent and φ a constant. We obtain the following expression for the characteristic exponent by introducing Eq.(30) into Eq.(29) and equating the coeffficients of $\sin n\tau$ and $\cos n\tau$ separately to zero:

$$\rho^2 = -(b_0 + n^2) + \sqrt{4n^2 b_0 + b_n^2}, \tag{31}$$

with $b_n^2 = b_{ns}^2 + b_{nc}^2$. From the transformation (28), we note that the stability of the control process is realized when $\eta(\tau)$ goes to zero in time so that the real part of $L \pm \rho$ should be negative. Since L must be real and positive, the amplitude of oscillations must satisfy the following condition:

$$\mu(1 - \frac{A^2}{2}) - 2\epsilon KU > 0. \tag{32}$$

Moreover, the stability of the system oscillations process is guaranteed if the following criterion is satisfied:

$$Q_n = (b_0 - n^2)^2 + 2(b_0 + n^2)L^2 + L^4 - b_n^2 > 0, \quad n = 1, 2, 3, 4. \tag{33}$$

$n = 1, 2, 3, 4$ represent the first, second, third and fourth parametric resonant states respectively. The fulfillment of the criteria (32) and (33) is essential to ensure the stability of the system oscillations. From the criterion (33) four parametric resonances are plotted as a function of the control parameter U. However the stability of the system will be obtained when criterion (32) will be satisfied. The effect of the parameters of the system on state of the second stability criterion for the four parametric resonances for $A = 0.56$ is observed in Figs. 12, 13, 14, 15, 16. It should be noted that whatever the conditions, the stability criteria are always satisfied for $n = 2, 3, 4$ but for $n = 1$ the instability domain appears and is influenced by certain parameters of the system. Fig. 12 presents the effects of linear restoring parameter α on the second stability domain and it can be observed that the instability domain increases with α for $\epsilon = 1$. In Fig. 13, we investigate the effect of the damping parameter μ for $\alpha = -0.5, \epsilon = 1$ and it is noticed that the stability increases with damping parameter μ. On the other hand, domains of U for which $Q_n < 0 (n = 1)$ lead to the occurrence of unstable oscillations are shown in Fig. 14 for the first parametric resonance. The influences of the parameters K and β on the stability of harmonic oscillation are addressed and results are shown in Figs. 15, 16, respectively. From Fig. 15 it is noticed that the stability domain decrases with the control parameter K and we can conclude that the control process is more stable for the low values of K. Through Fig. 16, one can notice that the constraint parameter β increases and deplaces the stability domain. We can conclude that the stability of harmonic oscillations is more achieved in the negative flow speed direction ($\epsilon = -1$) than the positive flow speed direction ($\epsilon = 1$).

4. Control of Chaotic dynamics states

The nonlinear chemical oscillations under consideration in this paper present the chaotic states which are often caused by instabilities. Our objective in this work is to suppress these undesirable phenomena by using the hydrodynamic control process. To achieve this goal, we use the fourth-order Runge Kutta algorithm to solve numerically Eq.(12) and the resulting bifurcation diagrams and its corresponding Lyapunov exponent are plotted when the amplitude of the fluctuating hydrodynamic drag forces F is varied. The bifurcation diagram and its corresponding Lyapunov exponent are obtained (see Fig. 17) in the absence of the control force ($\epsilon = 0$) and with the following parameters $\mu = 0.0001$, $\alpha = -0.5$, $\gamma = 0.05$, $\beta = 0.05$ and $\Omega = 1$. Now, we have always observed the presence of chaos in the system for $\epsilon = 1$ but the control process has reduced it (see Fig. 18) when the system is subjected to the action of hydrodynamic drag forces. We obtained the total disappearance of chaos when $\epsilon = -1$ (see Figs. 19, 20). By representing the phase portraits and its corresponding Poincaré sectin of the system at two different stages of the process for negative flow direction, we checked the efficiency of the passive control applied to the nonlinear chemical model. Thus, the phase portraits and its corresponding Poincaré section plotted in Figs. 21, 22 for appropriate choice of F and control parameters K and U confirmed the predictions of bifurcation diagrams and its corresponding Lyapunov.

5. Conclusion

In this paper, we have studied the nonlinear dynamics and passive hydrodynamics control of chemical oscillations modeled by a forced modified Van der Pol-Duffing oscillator. The model has been described and the corresponding equation of motion obtained. By using the Cardan method, we have determined the equilibrium points of autonomous system. The dynamical behaviors of system is qualitatively determined by evaluating the eigenvalues of corresponding Jacobian matrix at each of the equilibrium points. The second stability criteria is checked by using Floquet theory and Whittaker method. The numerical simulations are used to validated and complemented the results obtained by the analytical methods. We noted a more robust stability of oscillations in the negative flow speed direction than in the positive one. In both directions, the existence of instability zones is observed. We noticed also the increase or decrease of this instability area when certain parameters of the system increases or decrases. The effect of the control process on chaotic dynamic states has been effective with $\epsilon = -1$. The hysteresis phenomenon, jump amplitude of the harmonic oscillations and chaotic states have been successfully controlled by the passive hydrodynamic control sued in this work.

Acknowlegments

D. L. Olabodé thanks IMSP-UAC and DAAD for financial support. The authors thank Dr. Enjieu Kadji for his suggestions and collaborations. We would also like to thank very much the anonymous referees whose useful criticisms, comments and suggestions have helped strengthen the content and the quality of the paper.

References

[1] J. Boissonade, P. De Kepper, *Transitions from Bistability to Limit Cycle Oscillations. Theoretical Analysis and Experimental Evidence in an Open Chemical System,* J. Phys. Chem. 84(1980)501 − 506.

[2] A.M. Zhabotinskii, *Biological and Biochemical Osciihtws,* Academic Press, New York, 1972.

[3] I.R. Epstein, K. Showalter, *Nonlinear Chemical Dynamics: Oscillations, Patterns, and Chaos,* J. Phys. Chem. 100(1996)13132 − 13147.

[4] B.P. Belousov, *In Oscillations and Travelling Waves in Chemical Systems,* Wiley, New York, 1985.

[5] A.M. Zhabotinsky, F. Buchholtz, A.B. Kiyatkin, I.R. Epstein, I. Phys. Chern. 97(1993)7578.

[6] D. Zhang, L. Gyorgyi, W.R. Peltier, *Deterministic chaos in the Belousov-Zhabotinsky reaction: Experiments and simulations,* Chaos 3(4)(1993)723−745.

[7] F. Ali, M. Menzinger, *Stirring Effects and Phase-Dependent Inhomogeneity in Chemical Oscillations: The Belousov-Zhabotinsky Reaction in a CSTR,* J. Phys. Chem. A 101(1997)2304 − 2309.

[8] M. Bartuccelli, G. Gentile, J.A. Wright, *Stable dynamics in forced systems with sufficiently high/low forcing frequency,* Chaos, 26(2016)083108.

[9] H.G. Enjieu Kadji, J.B. Chabi Orou, R. Yamapi, P. Woafo, *Nonlinear dynamics and strange attractors in the biological system,* Chaos, Solitons and Fractals 32(2007)862 − 882.

[10] F. Kaiser, *Coherent modes in biological systems. In: Illinger KH, editor. Biological effects of nonionizing radiation,* A.C. S. Symp. Series, 157(1981).

[11] F. Kaiser, *Coherent excitations in biological systems: specific effects in externally driven self-sustained oscillating biophysical systems,* Springer-Verlag, Berlin Heidelberg, 1983.

[12] F. Kaiser, C. Eichwald, *Bifurcation structure of a driven multi-limit-cycle Van der Pol oscillator (I). The superharmonic resonance structure,* Int. J. Bifurcat. Chaos 485(1991)491 − 501.

[13] C.H. Miwadinou, A.L. Hinvi, A.V. Monwanou, J.B. Chabi Orou, *Nonlinear dynamics of a ϕ^6-modified Duffing oscillator: Resonant oscillations and transition to chaos,* Nonlinear Dyn. 88(2016)97 − 113.

[14] A.V. Monwanou, C.H. Miwadinou, C. Ainamon, J.B. Chabi Orou, *Hysteresis, quasiperiodicity and chaoticity in a nonlinear dissipative hybrid oscillator,* International Journal of Basic and Applied Sciences 7(2018)1 − 7.

[15] K. Hackl, C.Y. Yang, A.H.D. Cheng, *Stability, bifurcation and chaos of nonlinear structures with control-I. Autonomous case,* Int. J. Non-Linear Mech. 28(1993)441 − 454.

[16] R. Tchoukuegno, P. Woafo, *Dynamics and active control of motion of a particle in a ϕ^6 potential with a parametric forcing,* Physica D 86(2002)167.

[17] R. Tchoukuegno, B.R. Nana Nbendjo, P. Woafo, *Linear feedback and parametric controls of vibration and chaotic escape in a ϕ^6 potential,* Int. J. Non-Linear Mech. 38(2003)531 − 541.

[18] B.R. Nana Nbendjo, R. Yamapi, *Active control of extended Van der Pol equation,* Communications in Nonlinear Science and Numerical Simulation 12(2007)1550 − 1559.

[19] T.T. Soong, *Active structural control theory and practice,* John Wiley and Son, New York, 1990.

[20] B. Hess and A. Boiteux, *Mechanism of glycolytic oscillation in yeast. I. Aerobic and anaerobic growth conditions for obtaining glycolytic oscillation Hoppe Seylers,* Z. Physiol. Chem. 349(1968)1567 − 1574.

[21] L. von Klitzing, A. Betz, *Metabolic control in flow systems. I. Sustained glycolytic oscillations in yeast suspension under continual substrate infusion,* Arch. Mikrobiol. 71(1970)220 − 225.

[22] H.G. Enjieu Kadji, B.R. Nana Nbendjo, *Passive hydrodynamics control of plasma instabilities.* Commun. Nonlinear Sci. Numer. Simulat. 17(2012)1779 − 1794.

[23] C.H. Miwadinou, A.V. Monwanou, J. Yovogan, L.A. Hinvi, P.R. Nwagoum Tuwa, J.B. Chabi Orou, *Modeling nonlinear dissipative chemical dynamics by a forced modified Van der Pol-Duffing oscillator with asymmetric potential: Chaotic behaviors predictions,* Chinese Journal of Physics 56(2018)1089 − 1104.

[24] A. Shabunin, V. Astakhov, V. Demidov, A. Provata, F. Baras, G. Nicolis, V. Anishchenko, *Modeling chemical reactions by forced limit-cycle oscillator: synchronization phenomena and transition to chaos,* Chaos, Solitons and Fractals 15(2003)395 − 405.

[25] T. R. Mukundan, *Solution of cubic equations: An alternative method,* Resonance 15(4)(2010)347 − 350.

[26] A.H. Nayfey, D.T. Mook, *Nonlinear oscillations,* John Wiley and Sons, New York, 1979.

[27] C. Hayashi, *Nonlinear oscillations in physical systems,* McGraw-Hill Inc., New York, 1964.

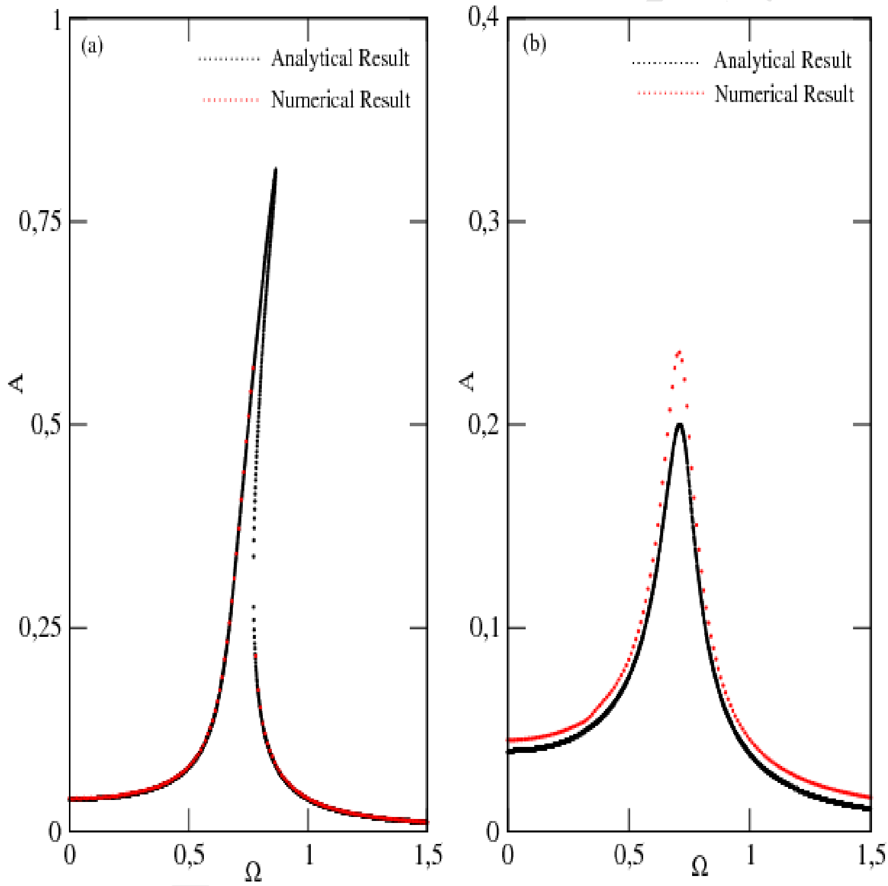

Figure 5: Comparaison between analytical and numerical frequency-response curve $A(\Omega)$ in the case (a) $\epsilon = 1; K = 0.05;\ U = 0.05$ (b) $\epsilon = -1;\ K = 1;\ U = 0.05$ with the parameters $\alpha = 0.5;\ \gamma = 0.5;\ \beta = 0;\ \mu = 0.04$ and $F = 0.02$.

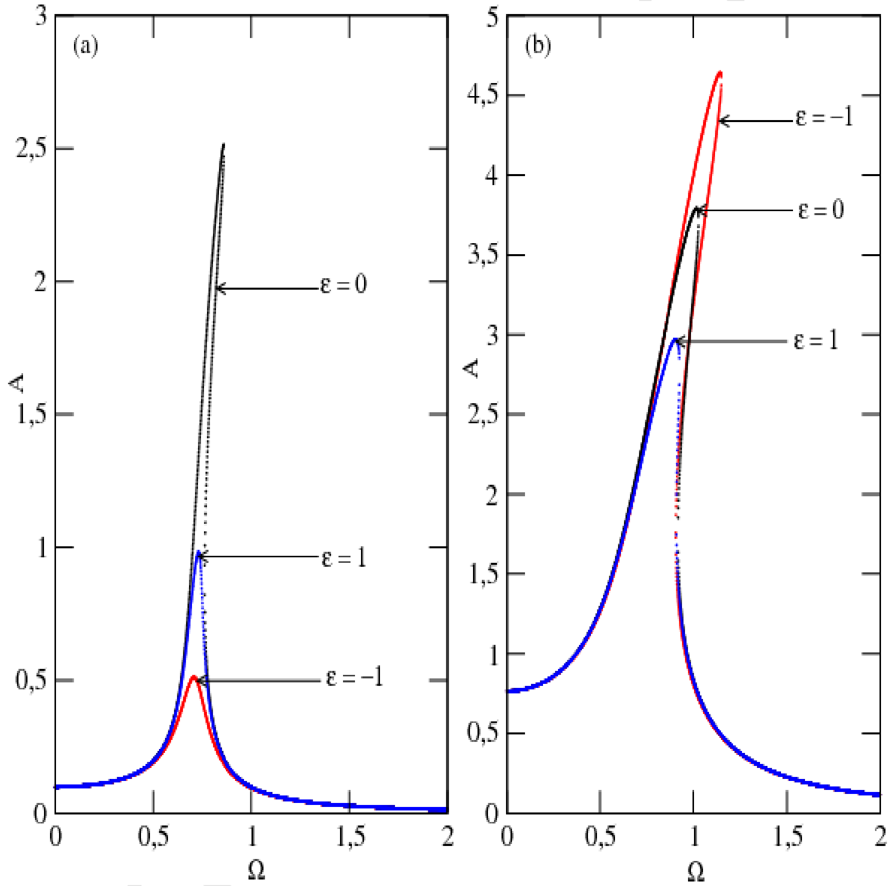

Figure 6: Effect of the control parameter ϵ on frequency-response curve in the case (a) $F = 0.05$ (b) $F = 0.4$ with the parameters $\alpha = 0.5$; $\gamma = 0.05$; $K = 1$; $U = 0.05$ and $\mu = 0.04$.

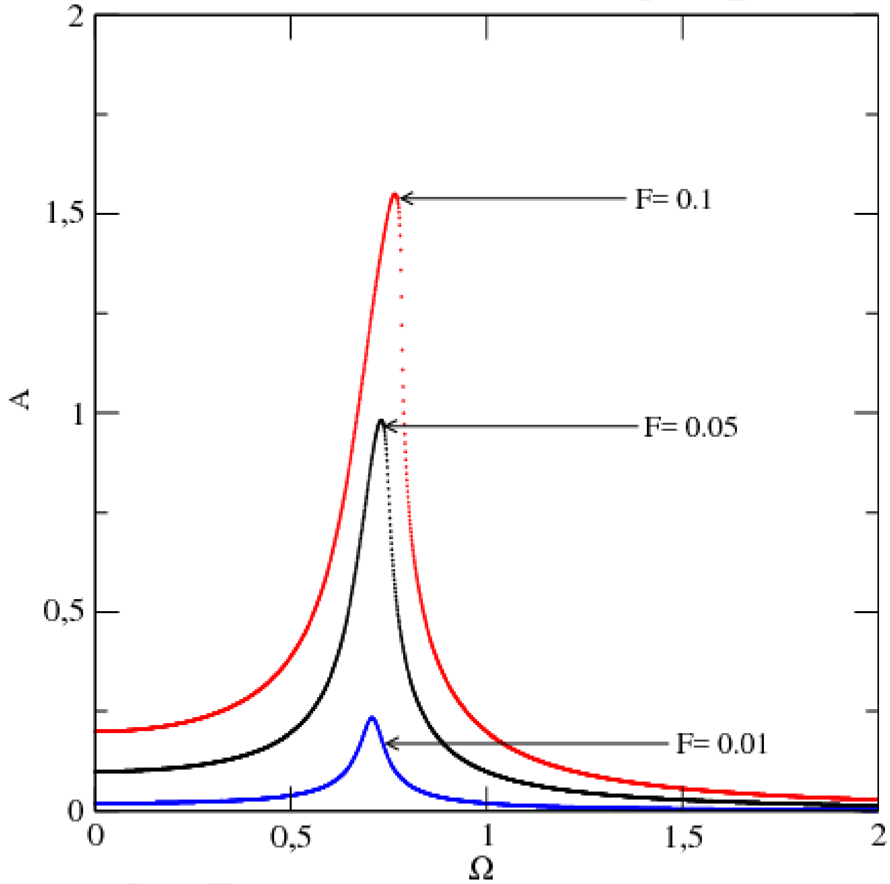

Figure 7: Effect of amplitude of external focing F on frequency-response curve with the parameters $\epsilon = 1$; $\alpha = 0.5$; $\gamma = 0.05$; $K = 1$; $U = 0.05$ and $\mu = 0.04$.

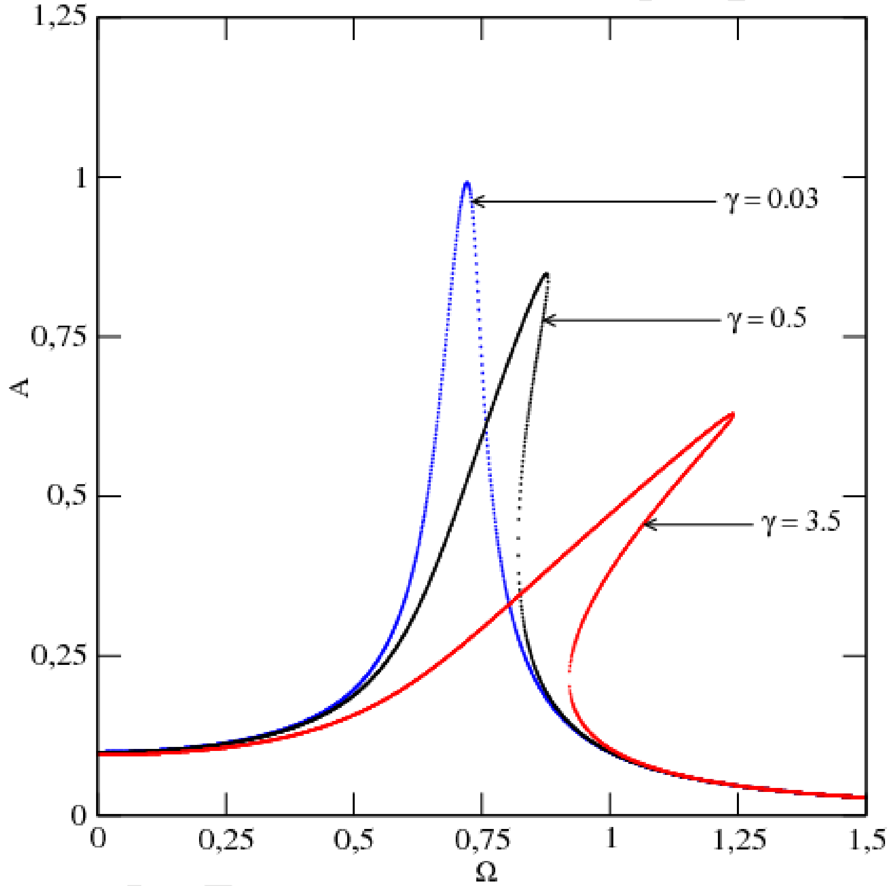

Figure 8: Effect of the parameter γ on frequency-response curve with the parameters $\epsilon = 1$; $\alpha = 0.5$; $K = 1$; $U = 0.05$ and $\mu = 0.04$ and $F = 0.05$.

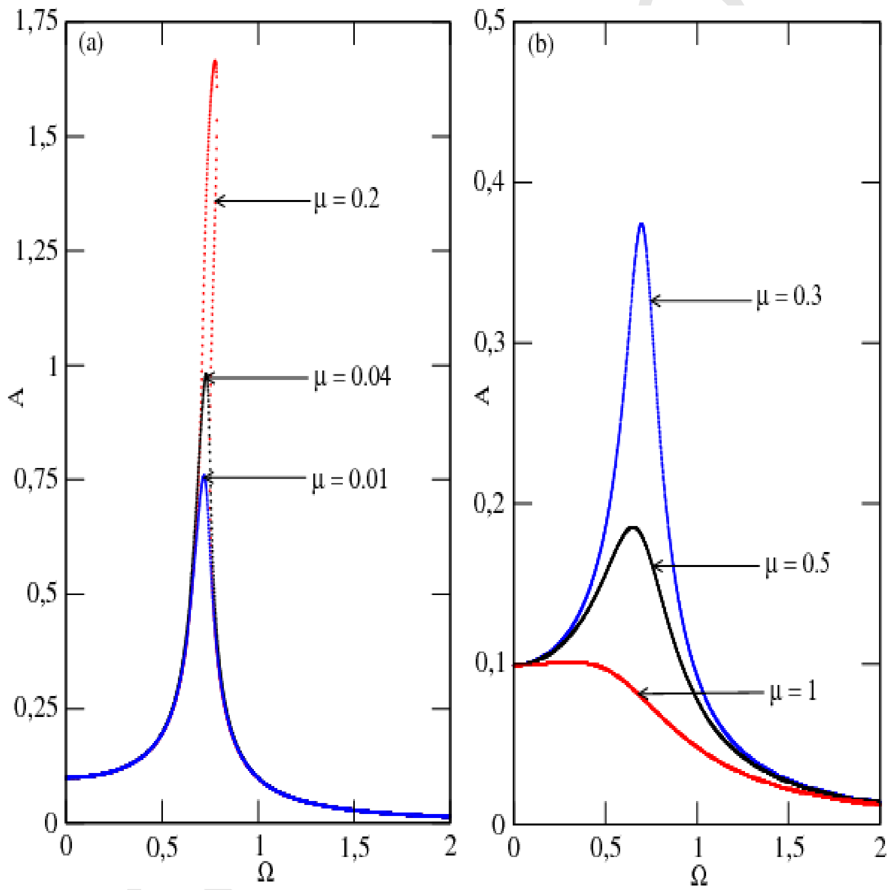

Figure 9: Effect of the parameter μ on frequency-response curve in the case (a) $\mu \leq 0.2$, (b) $\mu \geq 0.3$ with the parameters $\epsilon = 1$; $\alpha = 0.5$; $\gamma = 0.05$;$K = 1$; $U = 0.05$ and $F = 0.05$.

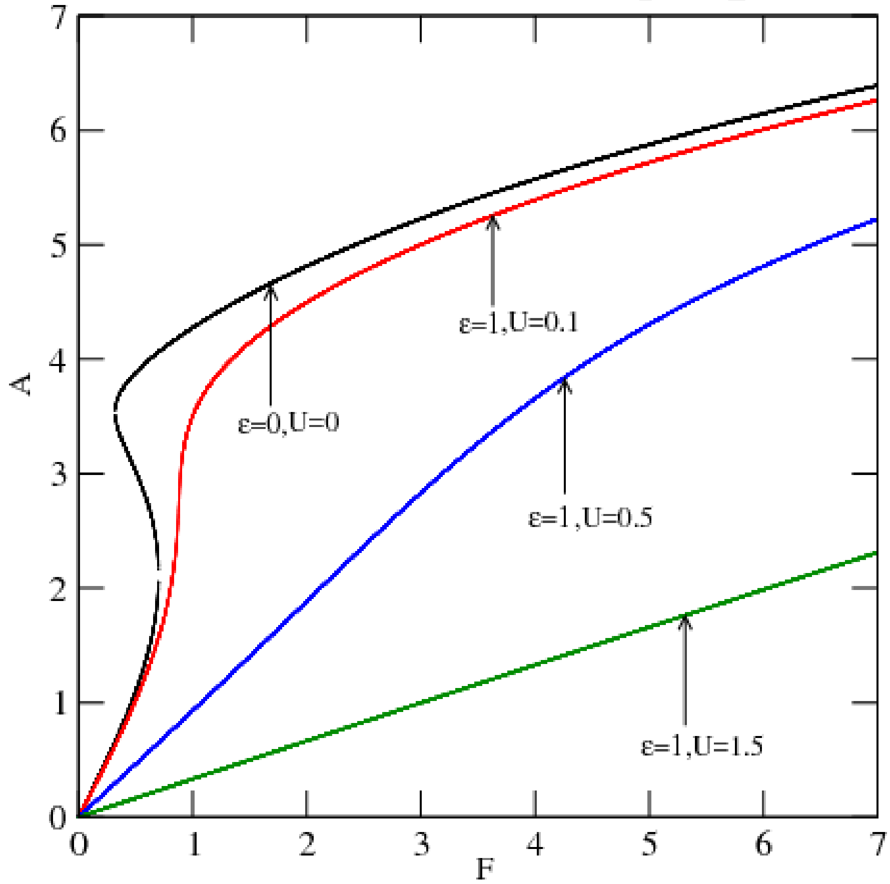

Figure 10: Effects of the control parameter U on the amplitude-response curve displaying jump in amplitude with the parameters $\alpha = 0.5$; $\gamma = 0.05$; $K = 1$; $\mu = 0.04$ and $\Omega = 1$.

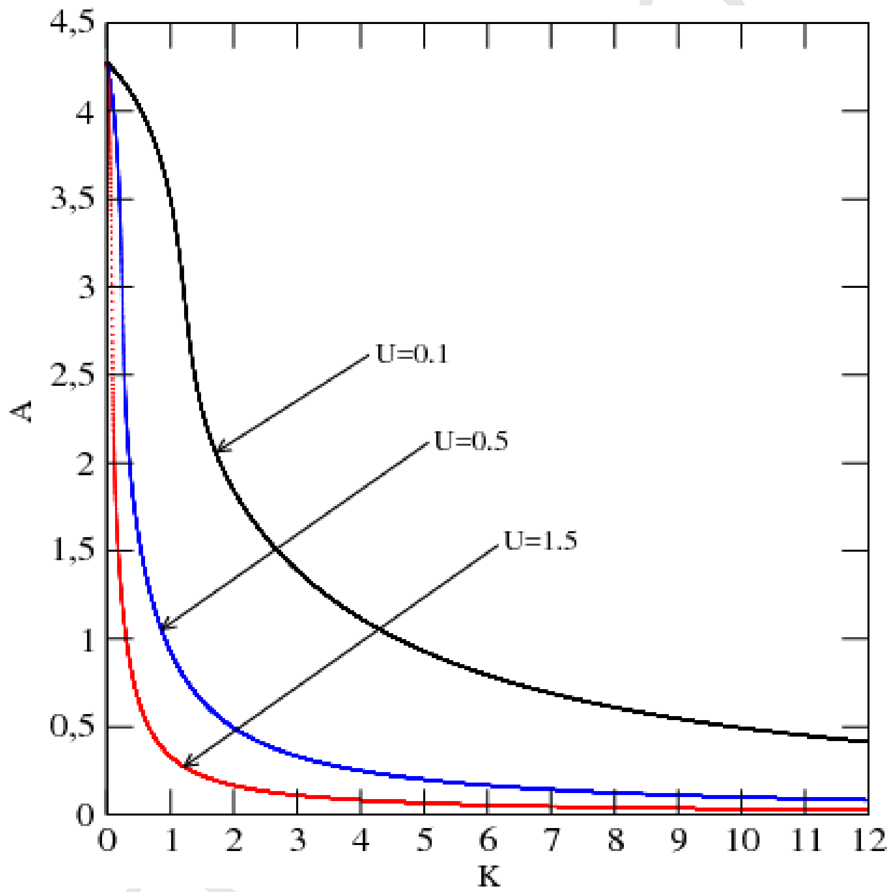

Figure 11: Effects of the coefficient U on the amplitude-response $A(K)$ with the parameters $\alpha = 0.5$; $\gamma = 0.05$; $\mu = 0.04$; $\Omega = 1$;$\epsilon = 1$ and $F = 1$.

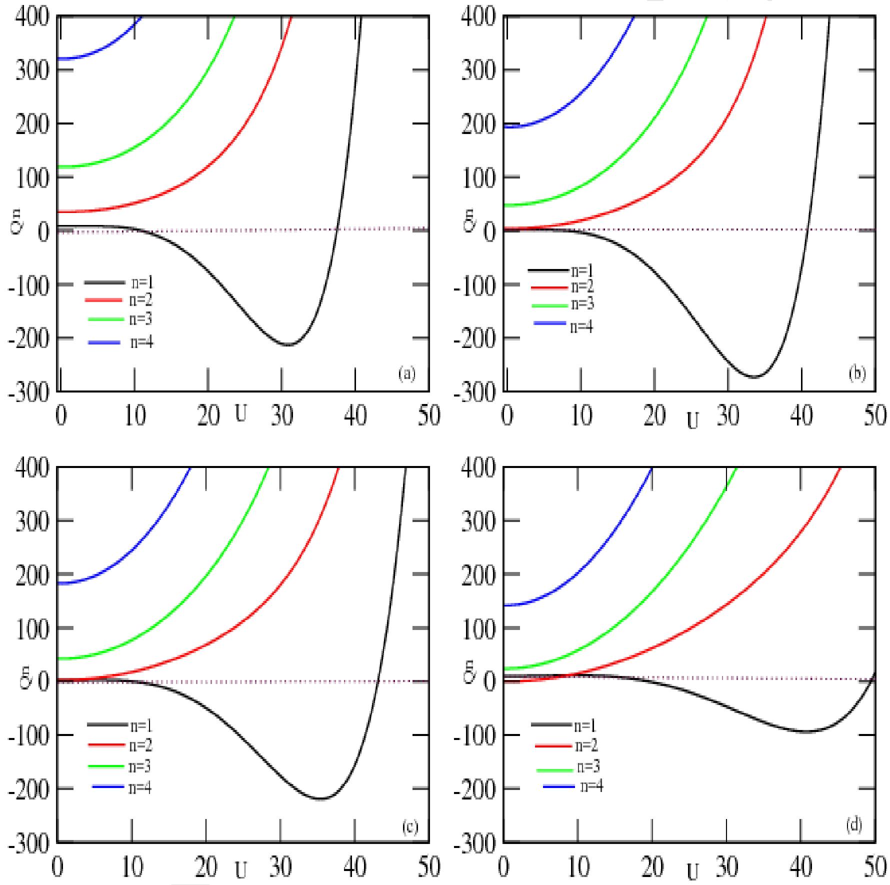

Figure 12: Effect of the parameter α on state of the second stability criterion for all the four parametric resonances for $A = 0.56$ and with the parameters: $\mu = 0.04$, $\gamma = 0.05$, $\beta = 0.05$, $K = 0.05$ and $\epsilon = 1$;(a) $\alpha = -0.5$; (b) $\alpha = 0.5$; (c) $\alpha = 0.60$; (d) $\alpha = 1$.

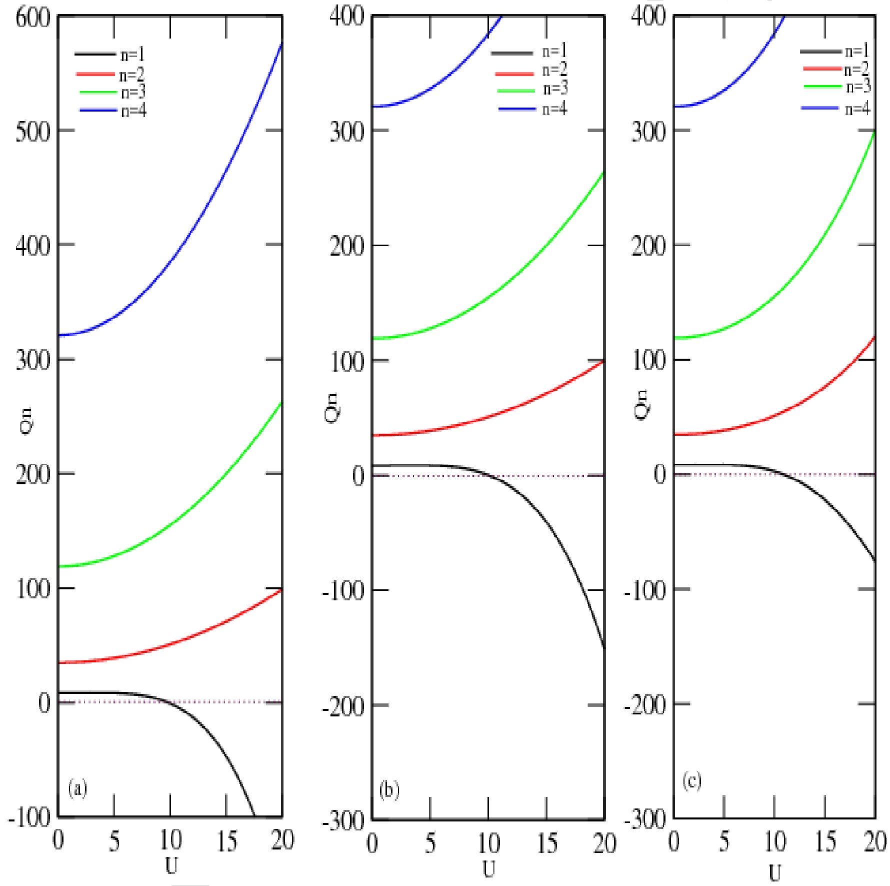

Figure 13: Effect of the parameter μ on state of the second stability criterion for all the four parametric resonances for $A = 0.56$ and with the parameters:$\gamma = 0.05$, $\beta = 0.05$, $K = 0.05$; $\alpha = -0.5$ and $\epsilon = 1$;(a) $\mu = 0.0001$; (b) $\mu = 0.01$; (c) $\mu = 0.04$.

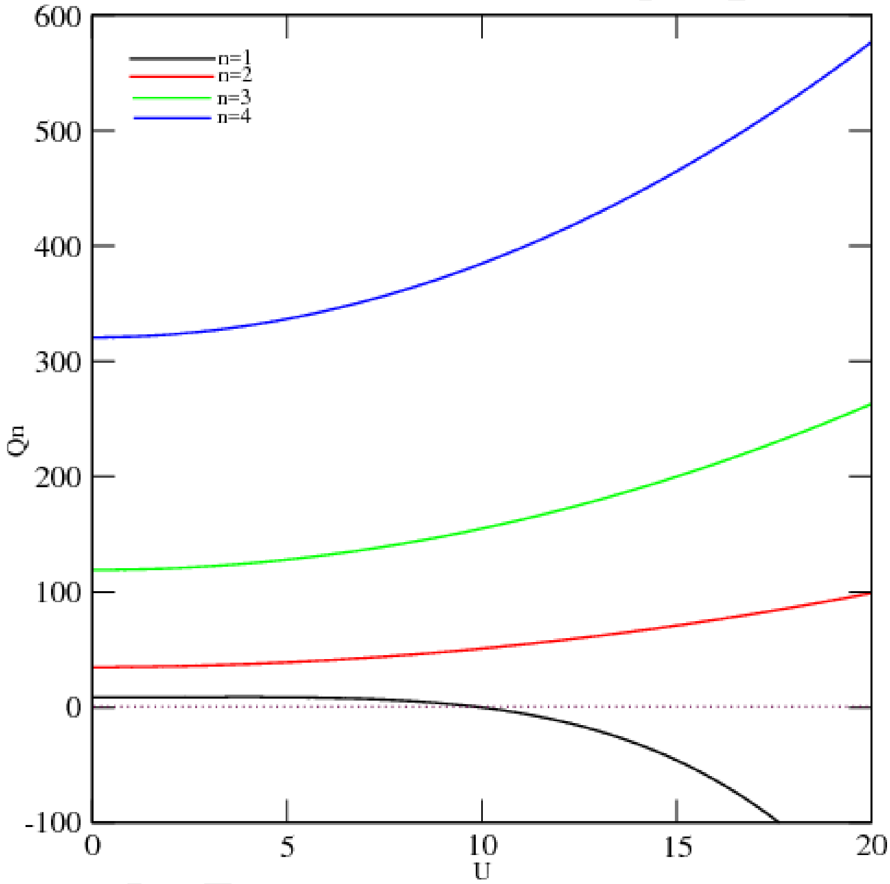

Figure 14: State of the second stability criterion for the first parametric resonance for $A = 0.56$ and with the parameters: $\mu = 0.0001$, $\alpha = -0.5$, $K = 0.05$, $\beta = 0.05$; $\gamma = 0.05$ and $\epsilon = -1$.

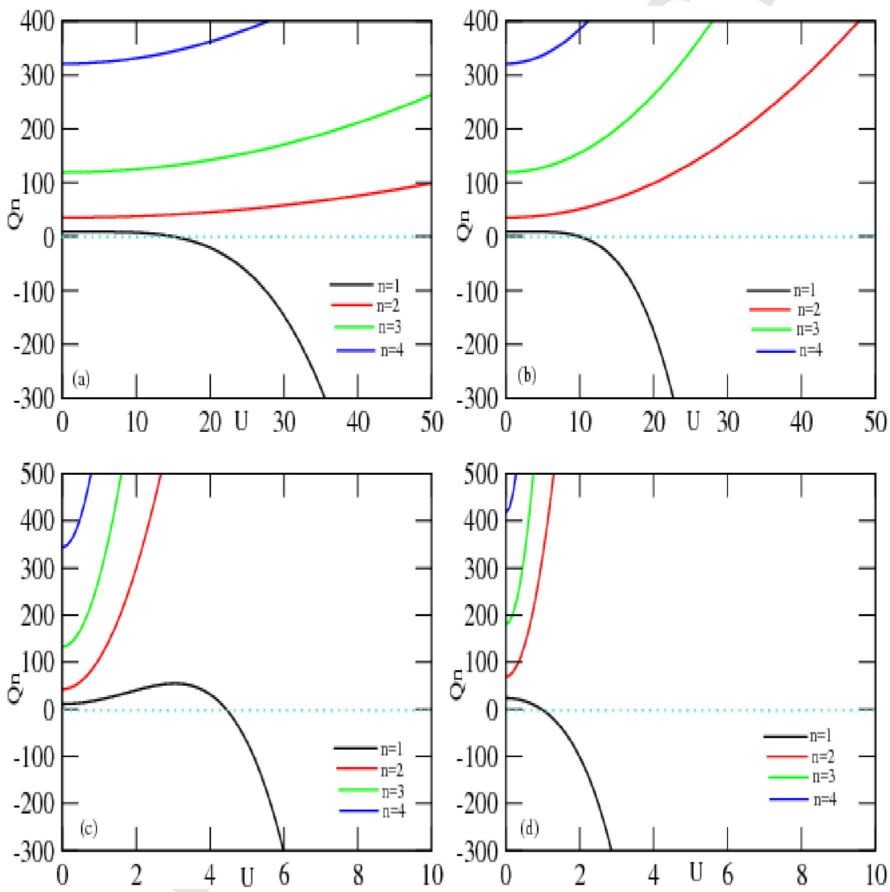

Figure 15: Effect of the parameter K on state of the second stability criterion for all the four parametric resonances for $A = 0.56$ and with the parameters: $\mu = 0.0001$, $\alpha = -0.5$, $\gamma = 0.05$, $\beta = 0.05$ and $\epsilon = -1$;(a) $K = 0.02$; (b) $K = 0.05$; (c) $K = 1$; (d) $K = 2$.

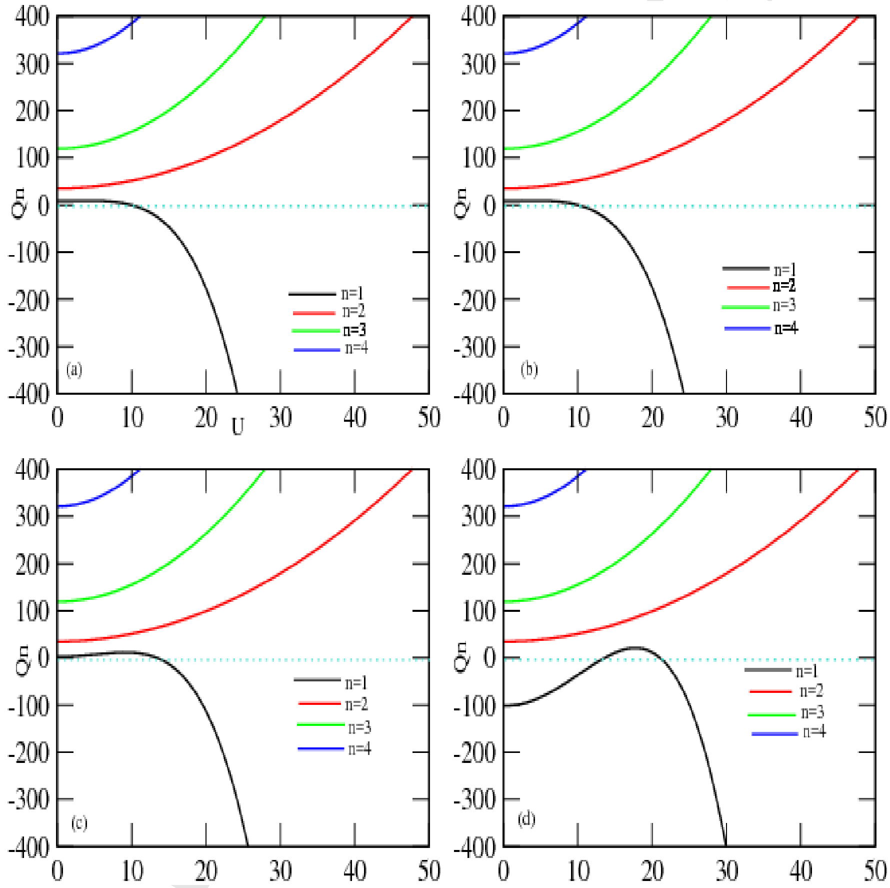

Figure 16: Effect of the parameter β on state of the second stability criterion for all the four parametric resonances for $A = 0.56$ and with the parameters: $\mu = 0.0001$, $\alpha = -0.5$, $\gamma = 0.05$, $K = 0.05$ and $\epsilon = -1$; (a) $\beta = 0$; (b) $\beta = 0.05$; (c) $\beta = 3.5$; (d) $\beta = 15$.

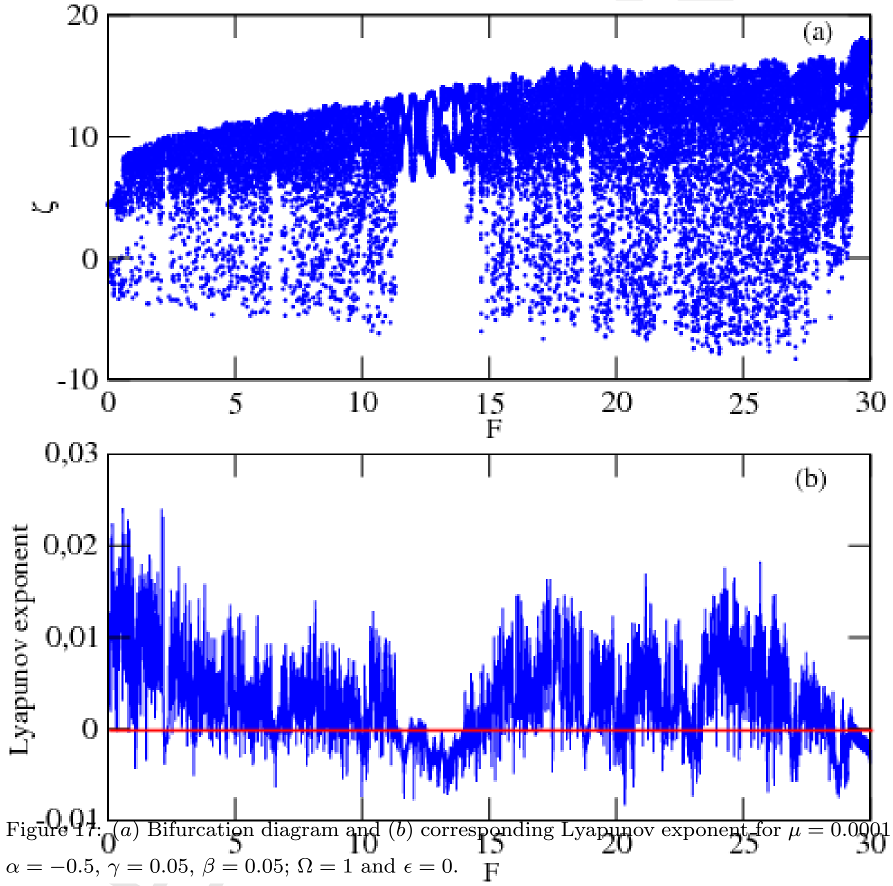

Figure 17: (a) Bifurcation diagram and (b) corresponding Lyapunov exponent for $\mu = 0.0001$, $\alpha = -0.5$, $\gamma = 0.05$, $\beta = 0.05$; $\Omega = 1$ and $\epsilon = 0$.

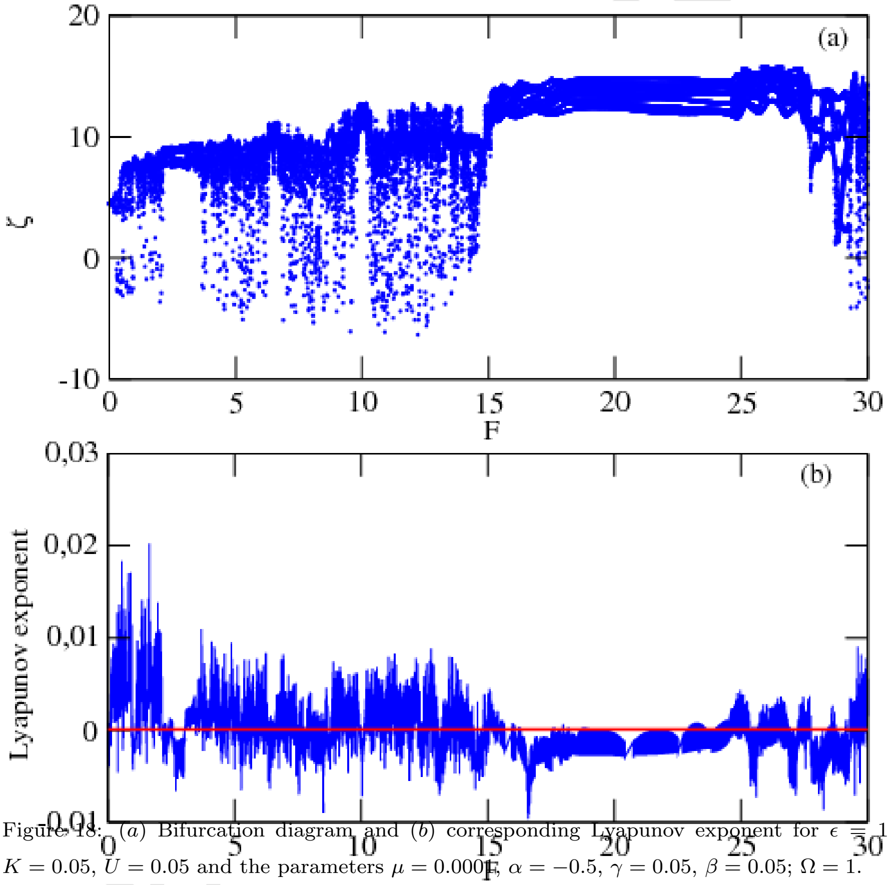

Figure 18: (a) Bifurcation diagram and (b) corresponding Lyapunov exponent for $\epsilon = 1$, $K = 0.05$, $U = 0.05$ and the parameters $\mu = 0.0001$, $\alpha = -0.5$, $\gamma = 0.05$, $\beta = 0.05$; $\Omega = 1$.

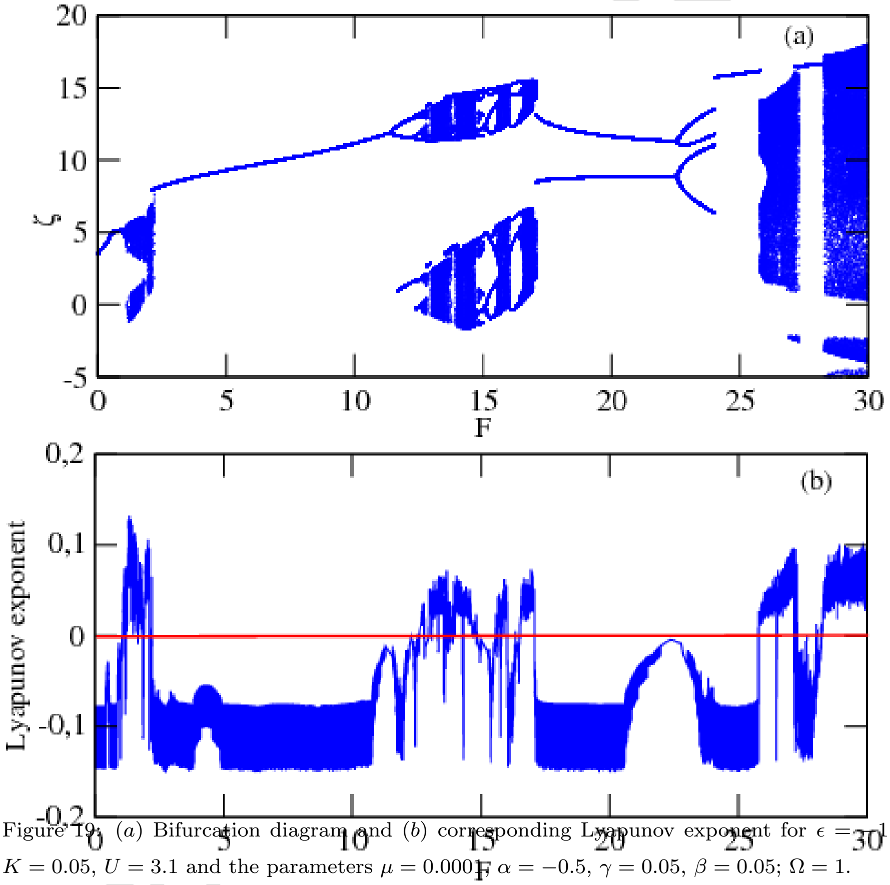

Figure 19: (a) Bifurcation diagram and (b) corresponding Lyapunov exponent for $\epsilon = -1$, $K = 0.05$, $U = 3.1$ and the parameters $\mu = 0.0001$, $\alpha = -0.5$, $\gamma = 0.05$, $\beta = 0.05$; $\Omega = 1$.

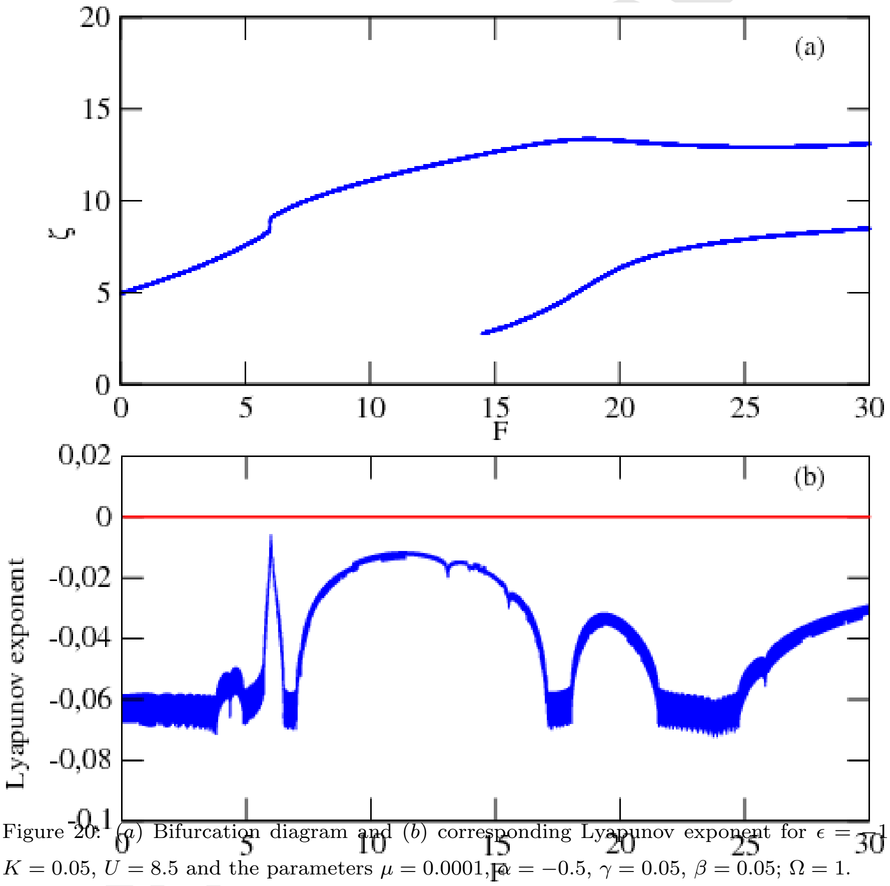

Figure 20: (a) Bifurcation diagram and (b) corresponding Lyapunov exponent for $\epsilon = -1$, $K = 0.05$, $U = 8.5$ and the parameters $\mu = 0.0001$, $\alpha = -0.5$, $\gamma = 0.05$, $\beta = 0.05$; $\Omega = 1$.

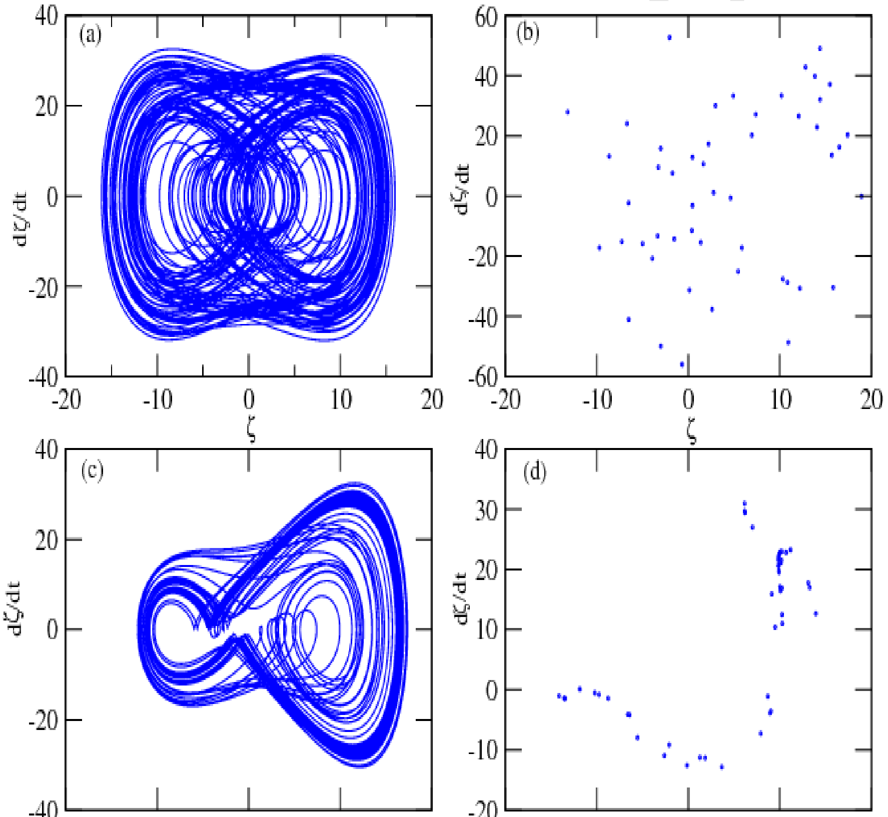

Figure 21: Chaotic phase portraits (left) and its corresponding Poincaré section (right) for the parameters $\mu = 0.0001$, $\alpha = -0.5$, $\gamma = 0.05$, $\beta = 0.05$; $\Omega = 1$;$F = 28.80$; (a),(b) $\epsilon = 0$ and(c), (d) effet of the control on chaos for $\epsilon = -1$, $K = 0.05$, $U = 3.1$.

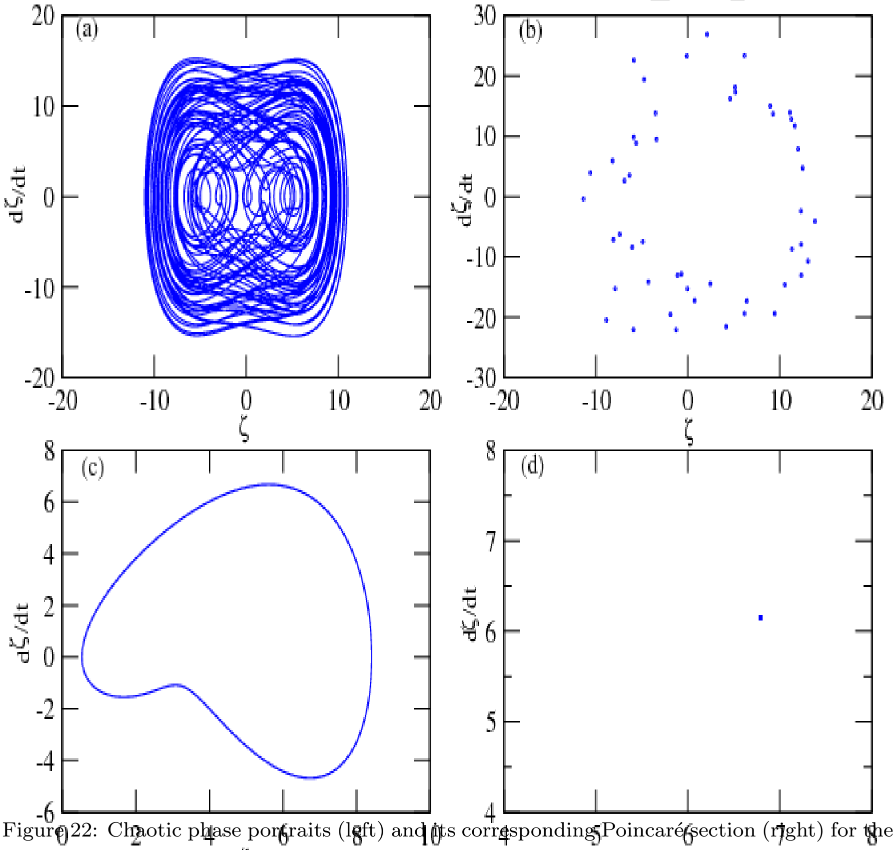

Figure 22: Chaotic phase portraits (left) and its corresponding Poincaré section (right) for the parameters $\mu = 0.0001$, $\alpha = -0.5$, $\gamma = 0.05$, $\beta = 0.05$; $\Omega = 1$;$F = 6$; (a),(b) $\epsilon = 0$ and(c),(d) effet of the control on chaos for $\epsilon = -1$, $K = 0.05$, $U = 8.5$.

Highlights

- Chaotic behaviors in a nonlinear chemical dynamics and its control are

Studied

- The passive hydrodynamic force is used to control the chaotic behaviors

- The stability of fixed points and harmonic oscillations is analyzed by using the appropriate methods

- Some effects of the news parameters are investigated numerically and

results are discussed

- Routes to chaos are investigated and efficiency of control force is studied